J|A|C|S ARTICLES

Published on Web 08/19/2010

Magnesium-Dependent Active-Site Conformational Selection in the Diels−Alderase Ribozyme

Tomasz Bereźniak,[†,‡] Maï Zahran,[†] Petra Imhof,*[,†] Andres Jäschke,[‡] and Jeremy C. Smith[†,§]

Computational Molecular Biophysics, IWR, University of Heidelberg, Im Neuenheimer Feld 368, 69120 Heidelberg, Germany, Institute of Pharmacy and Molecular Biotechnology, University of Heidelberg, Im Neuenheimer Feld 364, 69120 Heidelberg, Germany, and Oak Ridge National Laboratory, Post Office Box 2008 MS 6309, Oak Ridge, Tennessee 37831-6309

Received February 16, 2010; E-mail: petra.imhof@iwr.uni-heidelberg.de

Abstract: The Diels−Alderase ribozyme, an in vitro-evolved ribonucleic acid enzyme, accelerates the formation of carbon−carbon bonds between an anthracene diene and a maleimide dienophile in a [4 + 2] cycloaddition, a reaction with broad application in organic chemistry. Here, the Diels−Alderase ribozyme is examined via molecular dynamics (MD) simulations in both crystalline and aqueous solution environments. The simulations indicate that the catalytic pocket is highly dynamic. At low Mg^{2+} ion concentrations, inactive states with the catalytic pocket closed dominate. Stabilization of the enzymatically active, open state of the catalytic pocket requires a high concentration of Mg^{2+} ions (e.g., 54 mM), with cations binding to specific phosphate sites on the backbone of the residues bridging the opposite strands of the pocket. The free energy profile for pocket opening at high Mg^{2+} cation concentration exhibits a double minimum, with a barrier to opening of ∼5.5 kJ/mol and the closed state ∼3 kJ/mol lower than the open state. Selection of the open state on substrate binding leads to the catalytic activity of the ribozyme. The simulation results explain structurally the experimental observation that full catalytic activity depends on the Mg^{2+} ion concentration.

Introduction

Ribozymes, that is, ribonucleic acid enzymes, are capable of both catalyzing chemical reactions and storing genetic information.[1] These two features support the hypothesis of a preprotein "RNA world".[1−4] Ribozymes have been found in nature to mediate phosphodiester bond formation and cleavage and peptide bond formation reactions.[5−7] Further, artificial ribozymes have been shown to catalyze a broad array of other chemical reactions.[8,9] These findings suggest that in vitro-selected ribozymes may be regarded as analogues of the missing links in the transition from an RNA world to the present, protein-dominated life.[10] Among the artificial ribozymes, an in vitro-evolved Diels−Alderase ribozyme has been found to accelerate the formation of carbon−carbon bonds between anthracene dienes and maleimide dienophiles, presumably by a [4 + 2] cycloaddition reaction.[11] Catalysis proceeds with multiple-turnover catalytic reactions ($k_{cat} \approx 20$ min^{-1}) and high enantioselectivity (>95% enantiomeric excess) in a bimolecular fashion.[12] Reactions of this type, that is, creating simultaneously two new C−C bonds and up to four new stereocenters, have broad applications in organic chemistry and may have been essential in preprotein chemistry for a complex metabolism based on RNA.[13−19] The Diels−Alderase ribozyme is a 49-nucleotide RNA molecule that may also be converted into a bipartite system that consists of two strands, a 11-mer and a 38-mer (see Figure 1).

One of the principal features of RNA is its high negative charge density: one negative charge per nucleotide. Therefore, the presence of positively charged ions is essential for the

† Computational Molecular Biophysics, IWR, University of Heidelberg.
‡ Institute of Pharmacy and Molecular Biotechnology, University of Heidelberg.
§ Oak Ridge National Laboratory.

(1) Gilbert, W. *Nature* **1986**, *319*, 618.
(2) Zhang, B.; Cech, T. R. *Nature* **1997**, *390*, 96–100.
(3) Jeffares, D. C.; Poole, A. M.; Penny, D. *J. Mol. Evol.* **1998**, *46*, 18–36.
(4) Cech, T. R. *Cell* **2009**, *136*, 599–602.
(5) Cech, T. R. *Biochem. Soc. Trans.* **2002**, *30*, 1162–1166.
(6) Doudna, J. A.; Cech, T. R. *Nature* **2002**, *418*, 222–228.
(7) Steitz, T. A.; Moore, P. B. *Trends Biochem. Sci.* **2003**, *28*, 411–418.
(8) Jäschke, A.; Seelig, B. *Curr. Opin. Chem. Biol.* **2000**, *4*, 257–262.
(9) Lilley, D. M. J. *Curr. Opin. Struct. Biol.* **2005**, *15*, 313–323.
(10) Murray, J. M.; Doudna, J. A. *Trends Biochem. Sci.* **2001**, *26*, 699–701.
(11) Seelig, B.; Jäschke, A. *Chem. Biol.* **1999**, *6*, 167–176.
(12) Seelig, B.; Keiper, S.; Stuhlmann, F.; Jäschke, A. *Angew. Chem., Int. Ed.* **2000**, *39*, 4576–4579.
(13) Oikawa, H.; Katayama, K.; Suzuki, Y.; Ichihara, A. *J. Chem. Soc., Chem. Commun.* **1995**, *13*, 1321–1322.
(14) Oikawa, H.; Yagi, K.; Watanabe, K.; Honma, M.; Ichihara, A. *Chem. Commun.* **1997**, *1*, 97–98.
(15) Ichihara, A.; Oikawa, H. In *Comprehensive Natural Products Chemistry* Barton, D.; Nakanishi, K.; Meth-Cohn, O. , Eds.; Elsevier: Amsterdam: 1999; Chapt. I, pp 367−408.
(16) Auclair, K.; Sutherland, A.; Kennedy, J.; Witter, D. J.; Van den Heever, J. P.; Hutchinson, C. R.; Vederas, J. C. *J. Am. Chem. Soc.* **2000**, *122*, 11519–11520.
(17) Watanabe, K.; Mie, T.; Ichihara, A.; Oikawa, H.; Honma, M. *J. Biol. Chem.* **2000**, *275*, 38393–38401.
(18) Ose, T.; Watanabe, K.; Mie, T.; Honma, M.; Watanabe, H.; Yao, M.; Oikawa, H.; Tanaka, I. *Nature* **2003**, *422*, 185–189.
(19) Stocking, E. M.; Williams, R. M. *Angew. Chem., Int. Ed.* **2003**, *42*, 3078–3115.

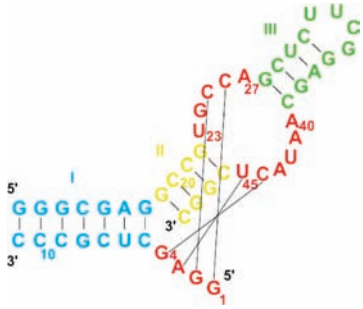

Figure 1. Secondary structure of the Diels−Alderase ribozyme. The ribozyme molecule consists of a 11-mer (5′-G1−3′-C11) and a 38-mer (5′-G12−3′-C49). Residues 23−27 and 40−45 form the asymmetric bulge segment. Solid black lines indicate Watson−Crick base-pairing between the 5′-G1-G2-A3-G4 segment and the residues from the opposite strands of the catalytic pocket. The 5′-G1-G2-A3-G4 segment plays a critical role in shaping both the RNA scaffold and the catalytic pocket. Colors mark the same domains as in Figure 2.

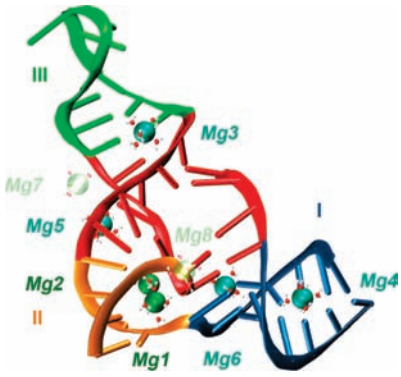

Figure 2. Crystal structure of the Diels−Alderase ribozyme stabilized by eight Mg^{2+} cations. Stems I−III are in blue, gold, and green, respectively. Residues forming and surrounding the nested catalytic pocket are marked in red. Mg1 and Mg2 (dark green spheres) make the most important contributions to the structural scaffold of the catalytic pocket. Mg3−Mg6 (light green) stabilize the λ-shaped RNA structure. Mg7 and Mg8 (transparent green) mediate contacts in the crystal lattice.

structural integrity and catalytic activity of all ribozymes.[20] The activity of the Diels−Alderase ribozyme was found to require divalent metal cations with similar physicochemical properties, that is, Ca^{2+}, Mn^{2+}, or Mg^{2+}, but no evidence for the direct involvement of metal ions in catalysis was detected.[11] Atomic force microscopy and anodic voltametry experiments are consistent with the Diels−Alderase ribozyme adopting a compact, stable, and tightly folded tertiary structure in the presence of magnesium cations.[21] Electron paramagnetic resonance spectroscopic investigations have indicated different affinities for five divalent metal ion binding sites.[22] Of the eight Mg^{2+} cations located in the ribozyme crystal structure (Figure 2), six participate in the stabilization of the RNA architecture (Mg1−Mg6) and the other two mediate contacts between ribozyme molecules in the crystal lattice (Mg7 and Mg8).[23] The Mg^{2+} ion named Mg2 makes the most important contribution

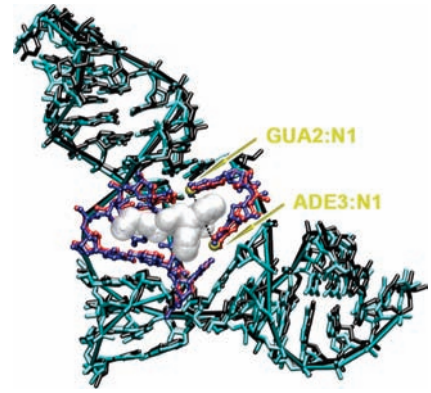

Figure 3. Crystal structures of the Diels−Alderase ribozyme in the unbound state (black) and in complex with the reaction product (cyan). Eight residues forming the core of the catalytic pocket in both states—GUA 2, ADE 3, URA 23, GUA 24, CYT 25, URA 42, ADE 43, and URA 45—are shown in red and blue, respectively. Dotted black line marks the present definition of the height of the catalytic pocket based on the binding interactions with the product in the crystal structure. Nitrogen atoms N1 of guanine 2 and adenine 3 are in yellow. Bound product is in silver.

to the structural scaffold of the catalytic pocket: the multiple contacts of this Mg^{2+} cation bridge the bases and sugar−phosphate backbones of six nucleotides situated at the bottom of the pocket. Moreover, Mg2, together with Mg1, mediates the packing of helices I and II against each other, stabilizing the bottom of the pocket. Mg3 and Mg5 stabilize the upper part of the pocket, whereas Mg4 and Mg6 are located in the groove of helix I.[23]

One of the characteristics originally attributed to the Diels−Alderase ribozyme was the existence of a preformed active site, there having initially been no experimental data indicating a major rearrangement in the RNA upon substrate binding. The preformed active site was inferred from chemical probing experiments[24] and then from the crystal structures of this ribozyme in the unbound state and complexed with the reaction product being nearly identical[23] (see Figure 3). However, both the chemical probing and X-ray analysis are static techniques and thus cannot reveal the dynamics of the system. Furthermore, the X-ray experiments were performed at a low temperature (100 K), severely restricting the dynamics, and moreover, the ribozyme was subjected to crystal packing constraints. Recent single molecule fluorescence resonance energy transfer (smFRET) and nuclear magnetic resonance spectroscopy (NMR) studies have revealed that in aqueous solution at room temperature the ribozyme is highly dynamic. The smFRET investigations revealed high conformational heterogeneity of the ribozyme at high Mg^{2+} ion concentrations.[25] Moreover, conformational dynamics involving transient opening of the catalytic pocket was proposed in the smFRET studies.[25] Further, NMR studies conducted in the presence of divalent cations confirmed that the whole asymmetric bulge segment (compare Figures 1 and 2) of an unbound ribozyme is highly dynamic in solution. Also, the rather poor NMR spectral resolution of the Mg^{2+}−ribozyme complex is again consistent with the presence of significant conformational fluctuations.[26]

The ribozyme's active site in the form of a catalytic pocket consists of eight residues that interact directly with substrate or

(20) Walter, N. G.; Engelke, D. R. *Biologist (London)* **2002**, *49*, 199–203.
(21) Chiorcea-Paquim, A. M.; Piedade, J. A. P.; Wombacher, R.; Jäschke, A.; Oliveira-Brett, A. M. *Anal. Chem.* **2006**, *78*, 8256–8264.
(22) Kisseleva, N.; Kraut, S.; Jäschke, A.; Schiemann, O. *HFSP J.* **2007**, *1*, 127–136.
(23) Serganov, A.; Keiper, S.; Malinina, L.; Tereshko, V.; Skripkin, E.; Höbartner, C.; Polonskaia, A.; Phan, A. T.; Wombacher, R.; Micura, R.; Dauter, Z.; Jäschke, A.; Patel, D. J. *Nat. Struct. Mol. Biol.* **2005**, *12*, 218–224.
(24) Keiper, S.; Bebenroth, D.; Seelig, B.; Westhof, E.; Jäschke, A. *Chem. Biol.* **2004**, *11*, 1217–1227.
(25) Kobitski, A. Y.; Nierth, A.; Helm, M.; Jäschke, A.; Nienhaus, G. U. *Nucleic Acids Res.* **2007**, *35*, 2047–2059.
(26) Manoharan, V.; Fürtig, B.; Jäschke, A.; Schwalbe, H. *J. Am. Chem. Soc.* **2009**, *131*, 6261–6270.

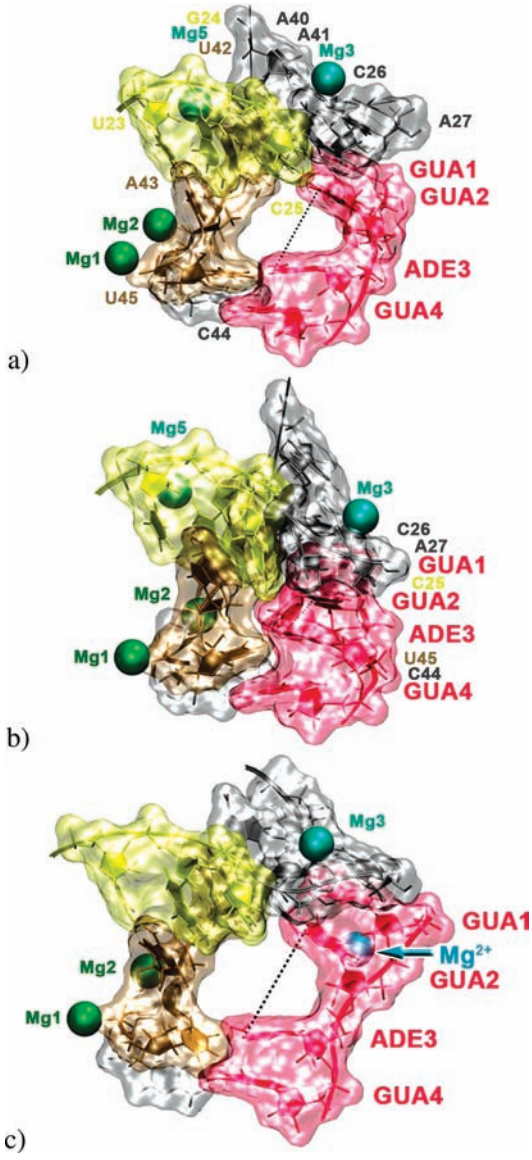

Figure 4. Catalytic pocket of the Diels−Alderase ribozyme. The 5′-G1-G2-A3-G4 segment is shown in red. Residues 23−25 and 42, 43, and 45 from the catalytic core are shown in yellow and tan, respectively. Residues surrounding the core are marked in gray. The crystallographic Mg^{2+} ions Mg1−Mg3 and Mg5 are in green. The dotted black line marks the present definition of the height of the catalytic pocket. (a) Catalytic pocket as found in the 1YKV crystal structure. The pocket height is 8.2 Å and the pocket volume is 317 $Å^3$. (b) Pocket in a closed state from simulation with eight Mg^{2+} ions. The height is 4 Å and the volume is 76 $Å^3$. (c) Pocket in an open state from simulation with 24 Mg^{2+} ions. The height is 11.2 Å and the volume is 330 $Å^3$. A noncrystallographic Mg^{2+} cation stabilizing the backbone of the G1 and G2 residues in that conformation is marked by the blue arrow.

product and a further seven residues from the asymmetric bulge segment that surrounds the catalytic core (Figure 4a). Note that it is the local conformation of the catalytic pocket which mainly determines whether the ribozyme can host its substrates and thus is active, as long as the global tertiary fold is maintained.

Given the highly dynamic nature of the Diels−Alderase ribozyme found in both smFRET[25] and NMR studies,[26] it is of particular interest to examine whether the initial interactions between the enzyme and a substrate induce a conformational change in the enzyme via "induced fit"[27] or, alternatively, the unbound enzyme exists as an ensemble of conformations in dynamic equilibrium, with the substrate interacting preferentially with one of these conformations, thus shifting the equilibrium in favor of the selected conformation.[28]

In this paper, we report molecular dynamics (MD) simulations of the Diels−Alderase ribozyme that probe the dynamic nature of the molecule at atomic detail. In particular, we examine the tertiary structure and catalytic pocket stabilization and thus the ribozyme's ability for substrate binding. Multiple 100 ns time scale MD simulations of the ribozyme in both the crystalline state and aqueous solution are reported, resulting in an overall microsecond sampling time. Simulations are performed at various temperatures and concentrations of Mg^{2+} ions. Particularly intriguing results are found concerning the magnesium-ion dependence of the active-site geometry. Understanding the local and internal conformational dynamics of the catalytic pocket provides insight into functional enzymatic properties of the ribozyme.

Methods

Crystal-State Molecular Dynamics Simulations. One aim of the crystal-state MD simulations is to mimic the conditions of the X-ray crystallographic measurements as closely as possible so as to enable a direct comparison with the experimental X-ray results. The crystal-state MD simulations at 100 K were performed at the temperature at which the X-ray measurements were carried out. Furthermore, these simulations provide a means of examining how the low experimental temperature inhibits the conformational dynamics of the ribozyme and affects the conformation of the catalytic pocket. The purpose of performing the crystal simulations at different temperatures is to determine at what temperature pronounced local conformational dynamics of the catalytic pocket is found or, alternatively, whether crystal packing constraints inhibit the active-site dynamics.

Molecular dynamics simulations of the crystal of the Diels−Alderase ribozyme in the unbound state, that is, without reactant or product in the catalytic pocket, were carried out. The initial structure was prepared by use of the CHARMM 32b2 package.[29] The potential energy function was the CHARMM nucleic acids force field parameter set 27[30] with the NAMD software.[31]

The unbound X-ray structure 1YKQ (Protein Data Bank) and the structure of the product complex 1YKV were determined at 3.5 and 3.3 Å resolution, respectively, and have been claimed to be virtually identical.[23] Indeed, the root-mean-square deviation (rmsd) between these structures is 0.81 Å, indicating very close structural similarity. Therefore, the slightly better-resolved structure 1YKV was chosen as the initial configuration for all simulations. The coordinates of four magnesium ions missing in both ribozyme molecules from the asymmetric unit were taken from the selenium-modified Diels−Alderase ribozyme structure (entry 1YLS, resolution 3.0 Å).

The resulting RNA structure with 8 Mg^{2+} ions in crystallographic positions was used to construct the crystal unit cell according to the experimental space group symmetry $P2_1$. The

(27) Koshland, D. E. *Proc. Natl. Acad. Sci. U.S.A.* **1958**, *44*, 98–104.
(28) Ma, B.; Kumar, S.; Tsai, C. J.; Nussinov, R. *Protein Eng.* **1999**, *12*, 713–720.
(29) Brooks, B. R.; Bruccoleri, R. E.; Olafson, B. D.; States, D. J.; Swaminathan, S.; Karplus, M. *J. Comput. Chem.* **1983**, *4*, 187–217.
(30) MacKerell, A. D.; Banavali, N.; Foloppe, N. *Biopolymers* **2000**, *56*, 257–265.
(31) Phillips, J. C.; Braun, R.; Wang, W.; Gumbart, J.; Tajkhorshid, E.; Villa, E.; Chipot, C.; Skeel, R. D.; Kalé, L.; Schulten, K. *J. Comput. Chem.* **2005**, *26*, 1781–1802.

four ribozyme molecules forming the crystal unit cell were solvated in 7059 TIP3P[32] water molecules and 140 sodium counterions were added, leading to an electrically neutral system of 28 730 atoms. Periodic boundary conditions were applied to mimic the full crystalline environment. Long-range electrostatic interactions were computed every 4 fs without any truncation by the particle mesh Ewald (PME) method,[33] for which the reciprocal sum was computed on a 80 Å × 45 Å × 80 Å grid with sixth-order interpolation and 1.5 Å Fourier grid spacing. Short-range electrostatics were computed at each time step without any truncation, and van der Waals interactions were computed every 2 fs with a smooth switching function between 8 Å and the cutoff value of 10 Å applied.

The system was first energy-minimized for 5000 steps by use of the conjugate gradient algorithm with the RNA atoms harmonically positionally restrained with a force constant of 1.0 kcal/mol·Å^2 and then gradually heated up to the experimental temperature with 1 K temperature steps and harmonic restraints. A first 25 ps equilibration run was performed in the NVE ensemble (with the number of particles, energy, and volume constant) with velocity rescaling applied. During the second and third equilibration runs, in the NPT ensemble, each 25 ps long, the system was kept at $T = 100$ K and $P = 1.01325$ bar. Temperature and pressure were controlled via the capabilities of NAMD: Langevin dynamics was used to maintain constant temperature, and the Nosé-Hoover Langevin piston[34,35] with a decay period of 500 fs was used for constant pressure. The restraints were gradually lifted from 0.5 through 0.25 to 0.05 kcal/mol·Å^2 during the three subsequent equilibration steps, respectively.

After the heating and equilibration, an NPT production run was performed without positional restraints. The integration time step was 2 fs, and covalent bond lengths involving hydrogen atoms were constrained by use of the SHAKE algorithm.[36] Coordinates were written every 2 ps. Before analysis, the coordinate sets of a trajectory were superimposed on a unit cell reference structure (the X-ray crystal unit cell structure) to remove overall unit cell rotation and translation. Production MD simulations were performed at 100 and 300 K for 100 ns and for 20 ns at temperatures of 150, 200, and 250 K.

Solution Molecular Dynamics. The solution molecular dynamics simulations allow the investigation of the ribozyme in the absence of crystal packing constraints and can permit comparison with the highly dynamic system found in both smFRET and NMR solution experiments.[25,26] In this model the main focus is on the direct dependence of the catalytic activity of the ribozyme on the Mg^{2+} ion concentration, suggested from experimental work[11] and here addressed from the structural point of view. The global and local conformational dynamics of the system are probed as a function of the concentration of Mg^{2+} ions. Stabilizing interactions between the negatively charged RNA and Mg^{2+} cations are characterized.

The starting structure for solution simulations of the Diels−Alderase ribozyme was obtained from the Protein Data Bank as described in the previous section. The MD simulations were performed at a temperature of 300 K for 100 ns (except where stated otherwise). A ribozyme molecule was prepared and centered in a cubic primary simulation cell with an initial box length of 90 Å by use of the CHARMM 32b2 package. In addition to the ribozyme and eight magnesium ions, 23 653 TIP3P water molecules and 32 sodium counterions, where not specified otherwise, were added, yielding an electrically neutral system comprising 72 581 atoms.

Five sets of ribozyme simulations at different Mg^{2+} ion concentrations and starting conditions were prepared as follows:

sim1: no divalent ions, with the system neutralized with 48 sodium counterions.

sim2: four magnesium ions, taken directly from X-ray structure 1YKQ (Mg1, Mg2, Mg3, and Mg7 in Figure 2), which is equivalent to a Mg^{2+} cation concentration of 9 mM, system neutralized with 40 sodium counterions.

sim3: eight magnesium ions, as found in the 1YKV crystal, a Mg^{2+} ion concentration of 18 mM, system neutralized with 32 sodium counterions; (**a**) open state or (**b**) closed state of the catalytic pocket as the starting structure.

sim4: 10 magnesium ions: eight Mg^{2+} cations in the crystallographic positions plus two noncrystallographic Mg^{2+} cations bridging phosphates groups of the 5′-G1-G2-A3-G4 segment, a Mg^{2+} ion concentration of 23 mM, system neutralized with 28 sodium counterions; (**a**) open state or (**b**) closed state of the catalytic pocket as the starting structure.

sim5: system neutralized with 24 magnesium cations (eight Mg^{2+} ions as found in the 1YKV crystal, 16 noncrystallographic Mg^{2+} ions positioned in the simulation box by replacing the water molecules at randomly chosen positions in the solvent bulk) and no additional counterions, equivalent to a Mg^{2+} ion concentration of 54 mM; (**a**) open state or (**b**) closed state of the catalytic pocket as the starting structure; (**c**) all 24 noncrystallographic Mg^{2+} ions positioned by replacing the water molecules at randomly chosen positions in solvent bulk, open state of the catalytic pocket as the starting structure.

All simulations were performed by use of the NAMD package with the CHARMM 27 nucleic acid force field and periodic boundary conditions. Long-range electrostatic interactions were computed every 4 fs without any truncation via the PME method, which the reciprocal sum computed on a 90 Å × 90 Å × 90 Å grid by use of sixth-order interpolation and 1.5 Å Fourier grid spacing. Short-range electrostatics were computed at each time step without any truncation, and van der Waals interactions were computed every 2 fs with a smoothing function between 8 Å and the cutoff value of 10 Å applied.

The system was energy-minimized, heated for 30 ps, and equilibrated with the number of particles, pressure (1.01325 bar), and temperature kept constant (NPT ensemble) during 3 × 25 ps equilibration time, by use of Langevin dynamics to maintain constant temperature and the Nosé-Hoover Langevin piston for constant pressure. The harmonic restraints were gradually lifted (0.5, 0.25, and 0.05 kcal/mol·Å^2) in the three equilibration steps. An integration time step of 2 fs was used and coordinates were saved with a sampling interval of 2 ps. The SHAKE algorithm was applied to constrain covalent bonds with hydrogen atoms. For the purpose of analysis, all coordinate sets of a trajectory were superimposed on a crystallographic reference structure to remove overall unit cell rotation and translation.

Restrained Molecular Dynamics Simulations. The restrained molecular dynamics simulations provide additional insight into the structural stabilization of the 5′-G1-G2-A3-G4 segment and

(32) Jorgensen, W. L.; Chandrasekhar, J.; Madura, J. D.; Impey, R. W.; Klein, M. L. *J. Chem. Phys.* **1983**, *79*, 926–935.
(33) Essmann, U.; Perera, L.; Berkowitz, M. L.; Darden, T.; Lee, H.; Pedersen, L. G. *J. Chem. Phys.* **1995**, *103*, 8577–8593.
(34) Martyna, G. J.; Tobias, D. J.; Klein, M. L. *J. Chem. Phys.* **1994**, *101*, 4177–4189.
(35) Feller, S. E.; Zhang, Y.; Pastor, R. W.; Brooks, B. R. *J. Chem. Phys.* **1995**, *103*, 4613–4621.
(36) Ryckaert, J.-P.; Ciccotti, G.; Berendsen, H. J. C. *J. Comput. Phys.* **1977**, *23*, 327–341.

the local dynamics of the catalytic pocket. The positional restraints on the phosphorus atoms in the backbones of the 5′-G1-G2-A3-G4 segment mimic their stabilization by Mg^{2+} ions. This model probes whether the structural stabilization of these phosphate groups alone suffices for transitions to occur between the closed (inactive) and open (active) states of the pocket. Moreover, the strength of the interactions stabilizing the pocket in an open state is evaluated by varying the magnitude of the restraints imposed.

As part of the analysis of the stabilizing effect of Mg^{2+} cations on the backbone, additional solution simulations were performed with positional constraints and restraints on the backbone of the residues that bridge the opposite strands of the catalytic pocket. The protocol was identical to the simulations in solution detailed above, except that in the 10 ns production runs either two or four selected phosphorus atoms from the nucleotide backbones were held constrained (their positions are fixed in space) or restrained (atoms can move from their positions to varying degrees based on the magnitude of the restraints). In the simulations with four harmonically restrained phosphorus atoms, the harmonic restraints were varied from 1.0 through 0.5, 0.1, to 0.09−0.01 kcal/mol·Å^2. Certain of these simulations were increased in length to 30−100 ns.

To determine whether the structural stabilization of backbones of the 5′-G1-G2-A3-G4 segment, here enforced by the restraints, is sufficient to obtain an open, active conformation of the catalytic pocket, all the simulations with harmonic restraints include only eight Mg^{2+} ions in crystallographic positions in order to maintain the overall tertiary fold.

Free Energy Calculations. For a system in thermodynamic equilibrium, the change in its free energy upon going from a reference state (ref) to a generic state *i* (e.g., from an open state of the catalytic pocket to a closed state) at constant temperature and constant pressure can be evaluated as the Gibbs free energy:

$$\Delta G_{\mathrm{ref}\rightarrow i} = -RT \ln \frac{p_i}{p_{\mathrm{ref}}} \tag{1}$$

where R is the ideal gas constant, T is the temperature, and p_i and p_{ref} are the probabilities of finding the system in state i and state ref, respectively.

Here, we describe the free energy surface as a function of the height of the catalytic pocket. We converted the probability distribution of being in a specific state, which means at a certain height of the catalytic pocket, to the free energy profile based on a Boltzmann distribution of the states of a system in MD simulation run. The free energy surface has been obtained from counting how often the system occurs in that state from an unbiased MD simulation trajectory: to obtain the free energy profile along the height of the pocket, the MD structures were projected onto 50 grid cells used to divide the overall range of an unbiased 90 ns MD simulation trajectory. Then the number of occurrences in a specific state was counted for every cell, and the relative probability density was calculated. The reference state was chosen to be the grid cell with the highest probability density, that is, the cell corresponding to the overall free energy minimum. Finally, the Gibbs free energy $\Delta G_{\mathrm{ref}\rightarrow i}$ was evaluated by use of eq 1.

The standard error of the mean quantifies the precision of the mean. It is a measure of how far the sample mean is likely to be from the true population mean. It takes into account both the value of the standard deviation and the sample size. The statistical error on the free energy profile evaluated from the simulation was estimated through the standard error of its mean, σ_{mean}, calculated over n subsets of the trajectory:

$$\sigma_{\mathrm{mean}} = \frac{\sigma}{\sqrt{n}} \tag{2}$$

$$\sigma = \sqrt{\frac{\sum_{i=1}^{n} (\bar{a}_i - \bar{a}^2)}{n-1}} \tag{3}$$

$$\bar{a} = \frac{\sum_{i=1}^{n} \bar{a}_i}{n} \tag{4}$$

where $\bar{a}_i$ is the mean of the height of the catalytic pocket evaluated in the ith subset and $\bar{a}$ and σ are the mean values over the n samples and the standard deviation, respectively. In the present case we used four subsets of one trajectory ($n = 4$), which was found to be a good compromise between the statistics within each subset and the sample size, n. If a normal distribution of the mean value $\bar{a}$ is assumed, the expected value of a is, with 95% confidence, inside the $\bar{a} \pm 2\sigma_{\mathrm{mean}}$ interval.

Hydrogen-Bond Analysis. Hydrogen-bond analysis was performed with the CHARMM 32b2 package. All hydrogen bonds were defined by two structural parameters. The first was a heavy atom donor−heavy atom acceptor distance with cutoff ≤3.5 Å. A second parameter, an angle off linearity, was measured as the complement of donor−hydrogen−acceptor angle. Thus, a linear hydrogen bond would be measured as a zero angle. The angular cutoff was ≤45°. The average occupancy was calculated as a ratio between the number of the trajectory frames with the hydrogen bond of interest formed and the total number of frames.

Structural Definition of the Catalytic Pocket Height. We define the height of the catalytic pocket as the distance between the guanine 2 nitrogen atom N1 (GUA2:N1) and adenine 3 nitrogen atom N1 (ADE3:N1) (see Figure 3). The present definition is based on the experimentally determined ribozyme−product binding interactions and suggested RNA−reactant interactions involving the anthracene aromatic ring intercalating between these two purines.[23]

The volume of the catalytic pocket was calculated by use of the CASTp server: http://sts.bioengr.uic.edu/castp/.[37]

All molecular images were prepared with the molecular visualization program VMD, version 1.8.6.[38]

Results

Crystal Simulations. Global and local dynamics of the Diels−Alderase ribozyme were examined by means of crystal-state molecular dynamics simulations in the experimental conditions of the X-ray crystallography measurement, as described in ref 23. To mimic these conditions as closely as possible, a 100 ns MD simulation was performed at 100 K for a crystal unit cell consisting of four ribozyme molecules with experimental space group symmetry and periodic boundary conditions. The unit cell dimensions were allowed to vary during the simulation and their average values, given in Table S1 of Supporting Information, were found to be close to the experi-

(37) Dundas, J.; Ouyang, Z.; Tseng, J.; Binkowski, A.; Turpaz, Y.; Liang, J. *Nucleic Acids Res.* **2006**, *34*, W116–W118.
(38) Humphrey, W.; Dalke, A.; Schulten, K. *J. Mol. Graph.* **1996**, *14*, 33–38.

mental values. After alignment of the MD coordinates with the X-ray structure, the root-mean-square deviation (rmsd) of the heavy atoms between the experimental and calculated structures was found to be 1.6 Å.

According to the experimental X-ray structures, the catalytic pocket architectures of the ribozyme in the free state and in the product complex are topologically very similar (Figures 3 and 4a). The height and volume of the catalytic pocket obtained from the 100 ns crystal simulation at 100 K are listed in Table S2 of Supporting Information. The volume of the catalytic pocket for the X-ray structure and that averaged from the crystal MD simulations are in good agreement. The difference between the height of the catalytic pocket in the experimental structure and the average obtained from the crystal MD simulations is 0.3 Å, indicating that only negligible changes in pocket height take place during the simulation. Moreover, all hydrogen bonds recognized in the X-ray structure as essential for the catalytic pocket were present for the entire simulation and never break (see Supporting Information for more details). Hence, at 100 K the experimentally observed open conformation of the catalytic pocket, which is able to host substrate and as such is catalytically active, is closely preserved.

The low experimental temperature of 100 K inhibits global dynamics of the ribozyme in general and strongly affects local conformational dynamics of the catalytic pocket region in particular (more details in Supporting Information). An additional simulation at 100 K starting from a closed state of the catalytic pocket, which is catalytically inactive since a diene reactant cannot be intercalated between the G2 and A3 purine rings, shows that the pocket remains in the closed conformation. Hence, both the open and the closed states are found to be stable at 100 K throughout the whole simulation time (100 ns each) when used as starting structures. However, 250 K was found to be high enough for collapse of the pocket (Figure S1 of Supporting Information). At 300 K, even in the crystalline state, transitions between the active and inactive states occur. Hence, the dynamic nature of the system becomes apparent only at high enough temperature, in agreement with the newest findings from smFRET[25] and NMR[26] experiments.

Dynamics of the Ribozyme in Solution. Magnesium Ion Dependent Structure and Dynamics. To obtain an insight into the dependence of the structural properties of the Diels−Alderase ribozyme on Mg^{2+} ions, four sets of molecular dynamics simulations in solution were carried out at different concentrations of these divalent cations: (1) **sim1**, no divalent ions; (2) **sim2**, four Mg^{2+} ions, which is equivalent to a Mg^{2+} cation concentration of 9 mM; (3) **sim3a**, eight Mg^{2+} ions (18 mM); and (4) **sim5a**, 24 Mg^{2+} cations (54 mM).

A strong influence of the Mg^{2+} ions on the ribozyme structure and dynamics was found. It is known from the X-ray structure that the 5′-G1-G2-A3-G4 segment plays a critical role in shaping both the RNA scaffold and the catalytic pocket.[23] Analysis of the MD trajectories revealed that, unlike in the X-ray structure, with zero Mg^{2+} ions the 5′-G1-G2-A3-G4 segment does not bridge the asymmetric bulge: there are no hydrogen bonds between the 5′-G1-G2-A3-G4 segment and two opposite strands of the asymmetric bulge and instead these two segments separate from each other. The MD structure differs significantly from the crystal structure in the 11-mer (5′-G1−3′-C11) segment (Figure 1), and the distance between the G2 and A3 purine rings averaged over the simulation time is too small (∼4 Å) for a diene reactant to sandwich in between. Furthermore, the overall tertiary fold is not maintained any more.

In the simulation with four Mg^{2+} ions, among which two cations are in the crucial crystallographic positions Mg1 and Mg2, the 5′-G1-G2-A3-G4 segment is closer to the asymmetric bulge. However, hydrogen bonds are formed mainly between residues G1 and C25, instead of between G1 and C26 as in the crystal, leading to the collapse of the catalytic pocket. The λ-shaped RNA structure is preserved.

In the simulation with eight Mg^{2+} cations, the 5′-G1-G2-A3-G4 segment is in an even closer position to the bulge than in the crystal structure. Hydrogen bonds are formed simultaneously between G1 and C26 and between G2 and C26 residues. However, stacking interactions between G2 and A3 result in the collapse of the catalytic pocket (the average distance between the G2 and A3 rings is 4 Å; see Figure 4b), and thus the ribozyme is again no longer able to host the substrate. Although the global structure of the eight Mg^{2+} ion simulation closely resembles the crystal structure, the pocket, which is local, is still closed for 95 ns out of the total 100 ns simulation time (see Figure 7a).

Finally, in the simulation at 54 mM Mg^{2+} ion concentration (i.e., 24 Mg^{2+} ions), all domains resemble the crystal structure, except the highly flexible region of the upper loop (residues 32−35 of helix III, see Figure S3 of Supporting Information). The 5′-G1-G2-A3-G4 segment bridges two opposite strands of the asymmetric bulge.

The average distances between the G2 and A3 purine rings in the simulations with zero, four, and eight Mg^{2+} ions are all ∼4 Å, corresponding to the closed state of the catalytic pocket. In contrast, only in the simulation with 24 Mg^{2+} ions is the average distance between the G2 and A3 rings ∼6.5 Å, corresponding to the open state of the pocket.

The MD simulations with zero, four, and eight crystallographic Mg^{2+} ions are consistent with the ribozyme being catalytically inactive at these relatively low concentrations, as the catalytic pocket is in the closed state. Interestingly, only in the simulation with 24 Mg^{2+} ions are several reopening events of the catalytic pocket observed when at least one noncrystallographic Mg^{2+} cation is in the proximity of the 5′-G1-G2-A3-G4 segment (Figure 4c). Thus, it seems that the local conformational dynamics of the catalytic pocket region, that is, possible transitions between the open and closed states, depends on the number of noncrystallographic Mg^{2+} ions. The key positions that must be occupied by these noncrystallographic Mg^{2+} ions are within binding distances of the phosphate groups of 5′-G1-G2-A3-G4 segment backbones (see Supporting Information for more details). In consequence, the experimentally observed highly dynamic nature of the system can be fully pronounced only at high enough Mg^{2+} ion concentrations.

Dynamics of the Catalytic Pocket. To carefully examine how Mg^{2+} ions interact structurally with the 5′-G1-G2-A3-G4 segment, shaping both the RNA scaffold and the catalytic pocket, an additional 100 ns simulation was performed, again with 24 Mg^{2+} ions (**sim5c**). This time all cations were randomly positioned in the solvent bulk by replacing the water molecules at randomly chosen positions. During this simulation, several collapsing−reopening events of the catalytic pocket were observed. Furthermore, almost all of the experimentally identified magnesium-binding sites were found to become occupied. Two Mg^{2+} ions bound to binding sites Mg1 and Mg2, which, on the basis of the X-ray structure, may contribute most to the stability of the structural scaffold.[23] Indeed, this MD structure resembles the crystal structure in all domains except the upper loop region. In contrast, no Mg^{2+} ions bound to the binding

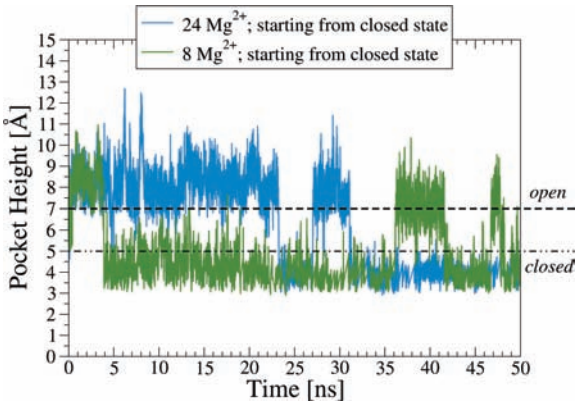

Figure 5. Height of the catalytic pocket versus simulation time from simulations in aqueous solution with eight Mg^{2+} ions (**sim3b**) and 24 Mg^{2+} ions (**sim5b**) starting from a closed conformation of the pocket.

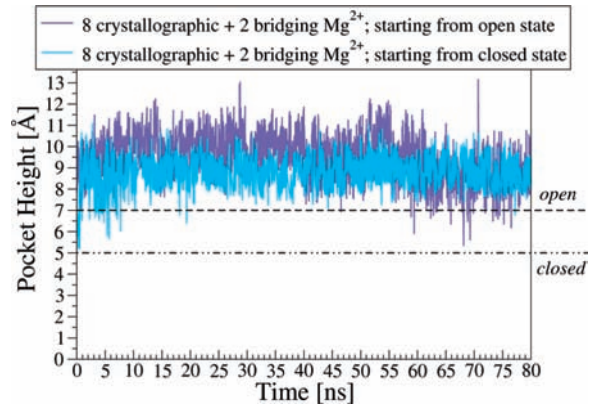

Figure 6. Height of the catalytic pocket versus simulation time from simulations in aqueous solution with eight crystallographic Mg^{2+} ions plus two noncrystallographic Mg^{2+} ions bridging the phosphate groups from the 5′-G1-G2-A3-G4 segment (**sim4a** and **sim4b**).

sites Mg7 and Mg8 that mediate contacts between RNA molecules in the crystal lattice. Mg^{2+} ions were also observed to be intermittently present at binding sites Mg3−Mg6. Interestingly, all of the random Mg^{2+} ions that ultimately diffuse to the crystallographically identified binding sites were initially positioned at least 20 Å apart from the occupied sites. Reopening of the catalytic pocket was observed only when at least one Mg^{2+} cation was in the proximity of the phosphate groups of the 5′-G1-G2-A3-G4 segment. These results suggest that local stabilization by Mg^{2+} ions of the backbone of these four crucial residues is the main determinant allowing reopening of the catalytic pocket.

In order to examine whether structural stabilization by Mg^{2+} ions indeed allows reopening of the catalytic pocket, two additional simulations were performed for 50 ns starting from closed conformations of the pocket, one with eight Mg^{2+} ions and one with 24 Mg^{2+} ions (**sim3b** and **sim5b**, respectively). In both these simulations, one of the crystallographic Mg^{2+} cations diffuses to the 5′-G1-G2-A3-G4 segment, where it binds to the phosphate groups and stabilizes the backbone, allowing reopening of the pocket. In the simulation with eight Mg^{2+} ions, the open state is reached but lasts only a few nanoseconds, while in the simulation with 24 Mg^{2+} ions, the open state is stabilized for more than 20 ns (Figure 5). This suggests increasing the concentration of Mg^{2+} ions increases the probability of binding interactions between cations and the 5′-G1-G2-A3-G4 segment backbone, permitting reopening and stabilization of the pocket in the open state.

In order to further characterize the preferred positions of the noncrystallographic Mg^{2+} ions, we have performed two additional 80 ns simulations, starting from the closed and open states, with eight Mg^{2+} ions in crystallographic positions and two noncrystallographic Mg^{2+} ions bridging the phosphate groups of the 5′-G1-G2-A3-G4 segment (**sim4a** and **sim4b**). In the corresponding simulation starting from the open state, the open conformation lasts for the whole simulation time and, moreover, the height of the catalytic pocket increases to 10 Å. In the simulation starting from the closed state, the pocket reopens after around 2 ns and stays in the reactive open conformation for the rest of the simulation time (see Figure 6). These results confirm that the presence of structural Mg^{2+} ions bound to the phosphate groups of the 5′-G1-G2-A3-G4 segment is crucial for the open state of the catalytic pocket. Higher concentrations of Mg^{2+} ions increase the probability of critical binding interactions between the cations and the 5′-G1-G2-A3-G4 segment phosphate groups.

In a further test of the 5′-G1-G2-A3-G4 segment backbone stabilization induced by the structural interactions with Mg^{2+} ions, several 10−30 ns long simulations were carried out with 5′-G1-G2-A3-G4 phosphorus atoms either fixed or harmonically restrained to their initial positions. These simulations include only eight Mg^{2+} ions in crystallographic positions in order to check whether the stabilization of 5′-G1-G2-A3-G4 segment backbones, here enforced by the restraints, is enough to obtain an open, active conformation of the catalytic pocket. Moreover, the strength of the interactions stabilizing the pocket can be evaluated from the magnitude of the restraints imposed.

In simulations in which only two particular phosphorus atoms, that is, those of the 5′-G1-G2 or G2-A3 or A3-G4 segment backbones, were fixed, a collapse of the catalytic pocket was found to still occur. The pocket remained in an active, open state only in the simulation in which all four phosphorus atoms of the 5′-G1-G2-A3-G4 segment were fixed.

Simulations were also performed with harmonic restraints of different strengths applied on the four phosphorus atoms of the 5′-G1-G2-A3-G4 segment. Here, a force constant of 0.09 kcal/mol·Å^2 was found to be high enough to prevent the collapse event during a 10 ns run. With force constants of 0.08−0.01 kcal/mol·Å^2 at least one reopening event was observed, and frequent collapse−reopening events were obtained when force constants were applied in the range of 0.06−0.01 kcal/mol·Å^2 for 30 ns simulation time.

Figure 7 shows a time series of the height and volume of the pocket from the simulation in solution with eight and 24 Mg^{2+} ions and the simulation with harmonic restraints of 0.01 kcal/mol·Å^2 for 100 ns. Pocket height and volume fluctuations of similar magnitude occur in these two simulations. Taken together, the above results indicate that the structural stabilization by Mg^{2+} cations of the backbone conformation of the residues in the 5′-G1-G2-A3-G4 segment by direct pairwise interaction is crucial for the stability of the open state.

Magnesium Cations Bound to Phosphate Groups of the 5′-G1-G2-A3-G4 Segment. In order to compare the number of Mg^{2+} cations structurally stabilizing the backbone of the 5′-G1-G2-A3-G4 segment in the simulations with eight and 24 Mg^{2+} ions (**sim3a** and **sim5a**, respectively), the radial distribution function (RDF) was calculated of Mg^{2+} ions around the corresponding center of mass of four backbone phosphorus atoms (Figure 8a).

The probability of finding Mg^{2+} cations within 4−6 Å of one of the backbone phosphorus atoms is at least 3 times higher

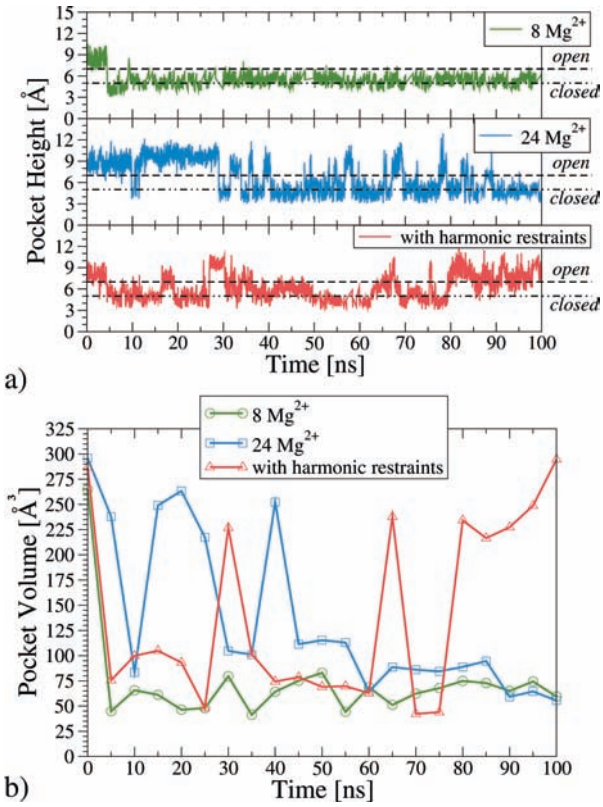

Figure 7. (a) Height and (b) volume of the catalytic pocket versus simulation time from simulations in aqueous solution with eight Mg^{2+} ions (**sim3a**), with 24 Mg^{2+} ions (**sim5a**), and with harmonic restraints on the phosphorus atoms of the 5′-G1-G2-A3-G4 segment of 0.01 kcal/mol·Å^2. In order to determine whether the structural stabilization of the backbone of the 5′-G1-G2-A3-G4 segment, here enforced by the restraints, is sufficient to obtain an open, active conformation of the catalytic pocket, all the simulations with harmonic restraints include only eight Mg^{2+} ions in crystallographic positions. The volume of the pocket was calculated periodically with a step of 5 ns between the snapshots.

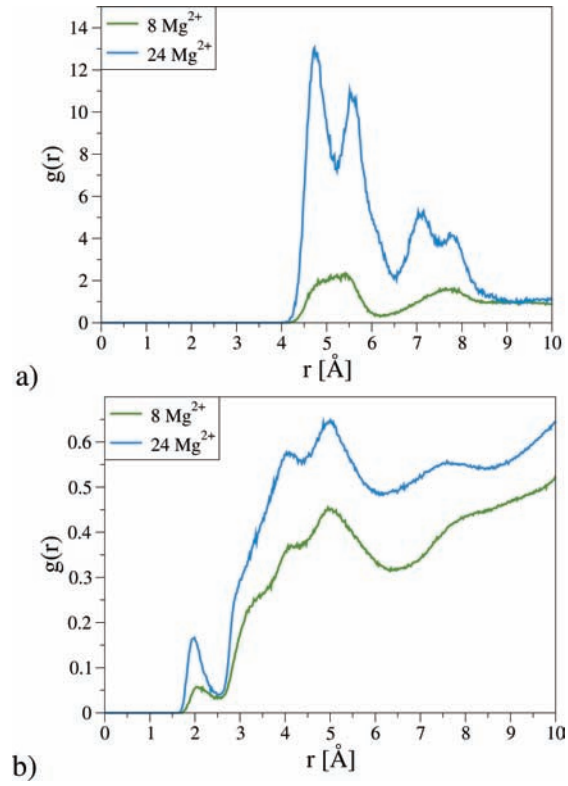

Figure 8. (a) Radial distribution function (RDF) of Mg^{2+} ions around the corresponding center of mass of the four backbone phosphorus atoms from the 5′-G1-G2-A3-G4 segment in solution simulations with eight and 24 Mg^{2+} ions (**sim3a** and **sim5a**, respectively). The probability of finding a Mg^{2+} cation within the range 4−6 Å is 3−6 times higher in the simulation with 24 Mg^{2+} ions than in the simulation with eight Mg^{2+} ions. At least 2 times higher probability is observed in the simulation with 24 Mg^{2+} ions for the distance of 7−8 Å. (b) RDF of water molecules around the center of mass of two nitrogen atoms N1 of guanine 2 and adenine 3, which define the height of the catalytic pocket, in simulations with eight and 24 Mg^{2+} ions (**sim3a** and **sim5a**, respectively). The most probable distance for finding a water molecule is around 5 Å in both simulation setups. The higher probability of finding water molecules in simulation with 24 Mg^{2+} ions reflects the longer residence of the water molecules in the open pocket conformation.

in the simulation with 24 Mg^{2+} ions than in the simulation with eight Mg^{2+} ions. Similarly, at least 2 times higher probability is observed in the simulation with 24 Mg^{2+} ions for the distance of 7−8 Å. In the crystal structure 1YLS, Mg^{2+} ions are found within the range of 3.5−5.5 Å from the phosphorus atoms, consistent with the first peak in the RDF. The peak at 7−8 Å may indicate interactions with a second shell of Mg^{2+} ions. Most likely, those more distant Mg^{2+} ions are more positionally disordered than the directly bound Mg^{2+} ions and as such are not resolved in the X-ray measurements.

Water Molecules within the Catalytic Pocket. In all simulations with an open conformation of the catalytic pocket as the starting-point structure, more than 10 water molecules were found within the pocket. In the simulations with eight Mg^{2+} ions, the water molecules remain in the pocket as long as it does not fully collapse. A collapse of the pocket is accompanied by replacement of the water molecules by the aromatic ring-stacking interactions and a subsequent rearrangement of the hydrogen-bond network. The closed state has no space for water molecules in the pocket (Figure 4b), although water molecules are still observed in the vicinity of the pocket. In the simulations with 24 Mg^{2+} ions, during a reopening event the water molecules are able to refill the pocket again and remain in it until the next collapse event takes place.

The probability of finding a water molecule at a distance of up to 10 Å from the center of mass of the two nitrogen atoms N1 of guanine 2 and adenine 3—that is, those atoms defining the height of the catalytic pocket in Figure 3—is presented as an RDF in Figure 8b. The most probable distance from the G2 N1 and A3 N1 atoms of finding a water molecule is around 5 Å in both simulation setups. However, the probability of finding water molecules in proximity to the N1 atoms (i.e., within the catalytic pocket) is higher in the case of simulation with 24 Mg^{2+} ions, reflecting the proportion of time the pocket is open. The number of water molecules residing within the catalytic pocket, calculated from the RDFs, is found to be 15 in the simulation with eight Mg^{2+} ions and 23 in the simulation with 24 Mg^{2+} ions. No Mg^{2+} ions were found within the catalytic pocket in any simulation.

Free Energy Calculations. By use of the probability distributions of the catalytic pocket height from the unbiased MD simulations, the corresponding Gibbs free energy profiles were calculated, and the results are shown in Figure 9.

The free energy profile obtained from the simulation in solution with eight Mg^{2+} ions possesses only one, closed-state minimum at 5.0 Å. However, the simulation with 24 Mg^{2+} ions possesses two minima: one at 3.6 Å (closed pocket) and a second one at 7.8 Å (open pocket). The free energy barrier to opening is 5.5 kJ/mol, and the difference between the minima is 2.9

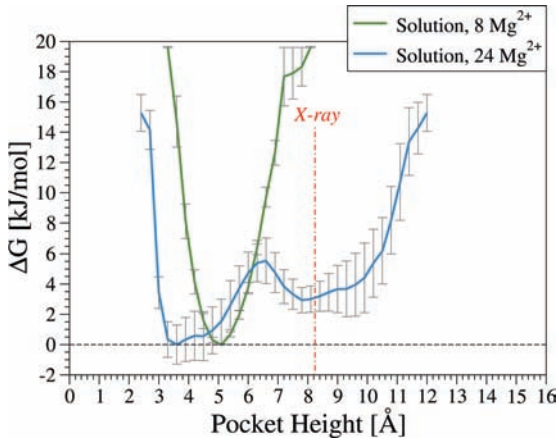

Figure 9. Gibbs free energy versus height of the catalytic pocket from the simulations with eight and 24 Mg^{2+} ions in solution (**sim3a** and **sim5a**, respectively). Each free energy profile was evaluated on the basis of the last 90 ns of an unbiased 100 ns MD simulation trajectory. The height of the pocket observed from the X-ray experimental structure is marked by a red line.

Table 1. Hydrogen-Bond Network for the 5′-G1-G2-A3-G4 Segment in Different Simulation Conditions[a]

		avg occupancy (%)			
		crystal	solution		
donor	acceptor	8 Mg^{2+}	8 Mg^{2+}	24 Mg^{2+}	restraint
G1 N2	C26 O2[b]	26	5	77	54
G1 N1	C26 N3[b]	3	0	5	57
G1 N1	A27 N3	0	91	1	0
C26 N4[b]	**G1** O6	25	97	4	12
G2 N2	C25 O2[b]	24	4	22	12
G2 N2	C26 O2	9	95	14	17
G2 N2	C26 N3	0	83	4	1
G2 N2	C25 N3[b]	29	4	23	17
G2 N1	C26 O2	8	90	24	16
G2 N1	C26 N3	1	92	4	3
C25 N4[b]	**G2** O6	21	73	16	22
A3 N6	U45 O4[b]	0	70	0	73
U45 N3[b]	**A3** N1	3	100	32	100
G4 N2	C44 O2[b]	95	97	61	98
G4 N1	C44 N3[b]	58	92	55	94
C44 N4[b]	**G4** O6	60	99	43	86

[a] Simulations in solution: 8 Mg^{2+}, **sim3a**; 24 Mg^{2+}, **sim5a**. Residues from the 5′-G1-G2-A3-G4 segment are shown in boldface type. [b] Hydrogen bonds suggested by the experimental X-ray structure 1YKV.

kJ/mol. The relatively low energy barrier and the low energy difference between the minima permit reversible transitions between the catalytically inactive and active states.

Although the free energy profile, shown in Figure 9, represents only local sampling, the barrier for the transition from a closed to an open pocket conformation in the case of eight Mg^{2+} ions can be estimated to be significantly higher than in the simulation with 24 Mg^{2+} ions and the open pocket conformation to be only rarely populated.

Hydrogen Bonding within the Catalytic Pocket. Finally, we analyze the hydrogen-bond network for the 5′-G1-G2-A3-G4 segment that bridges the opposite strands of the pocket (residues G2 and A3 define the pocket height). The results are presented in Table 1.

The hydrogen-bond occupancies for the 5′-G1-G2-A3-G4 segment indicate that, in the solution simulations with eight Mg^{2+} ions, a rearrangement in the hydrogen-bond network takes place relative to that seen crystallographically. The most significant examples of this are residue G2, which forms hydrogen bonds mainly with C26 instead of C25 as in the X-ray structure, and residue G1, which forms hydrogen bonds not only with residue C26 but also with A27. This alternative base pairing with high occupancies is observed mainly for conformations with the catalytic pocket closed (see Figure 4b). In simulations where reopening of the pocket is observed, the occupancies for G2−C26 and G1−A27 bonds are significantly lower and hydrogen bonds are formed mainly between those base pairs seen experimentally. This suggests that the catalytically inactive conformation is stabilized by a specific hydrogen-bond network within the pocket.

Discussion

Crystal-state simulations of different states of the catalytic pocket at 100 K result in a static picture of the system with no conformational rearrangements permitted. Both possible states, open and closed, of the catalytic pocket are independently stabilized on the ∼100 ns time scale depending on the starting structure. It was conceivable that the crystal lattice would prevent pocket opening and closing even at 300 K. However, 250 K was found to be high enough for collapse of the pocket, and at 300 K even in the crystalline state some transitions between the active and inactive states occur. Hence, the dynamic nature of the system becomes apparent only at high enough temperature, in agreement with the newest findings from smFRET and NMR experiments.[25,26] The low-temperature crystal simulations demonstrate why the functional dynamics could not be observed crystallographically. Higher temperature simulations in the crystalline state permit us to determine that pocket opening and closing is still possible in the presence of crystal contacts. The resolution of the experimental crystallographic structures does not permit an unambiguous assignment of the positions of the atoms forming the pocket, such that the presence of both conformations, open and closed, is conceivable.

The smFRET investigations revealed high conformational heterogeneity of the Diels−Alderase ribozyme at high Mg^{2+} ion concentrations.[25] Moreover, conformational dynamics of the catalytic pocket based on its transient opening was proposed in these investigations. Furthermore, NMR spectroscopic studies of the ribozyme have shown that the asymmetric bulge segment is highly dynamic in solution, and this is a feature common to some other ribozymes (e.g., the hammerhead ribozyme[39]). Also, the rather poor NMR spectral resolution of the Mg^{2+}−ribozyme complex is consistent with the presence of significant conformational fluctuations.[26] Our solution molecular dynamics simulations allow the investigation of the ribozyme in the absence of crystal packing constraints and can permit comparison with the highly dynamic system found in both smFRET and NMR solution experiments. In the solution simulations at high enough Mg^{2+} ion concentration, the system reveals fully its highly dynamic nature.

The simulations with 24 Mg^{2+} ions, including the simulation performed with the cations randomly positioned in the solvent bulk and the simulation with a closed state as the starting-point structure, demonstrate a direct correlation between the probability of the catalytic pocket being open and the probability of Mg^{2+} cations being bound to the phosphate groups of the 5′-G1-G2-A3-G4 segment backbone. This structural stabilization of the backbone architecture of the 5′-G1-G2-A3-G4 residues is crucial for stabilization of the catalytic pocket in an open

(39) Blount, K. F.; Uhlenbeck, O. C. *Annu. Rev. Biophys. Biomol. Struct.* **2005**, *34*, 415–440.

conformation. Furthermore, the simulation with zero Mg^{2+} ions (i.e., with 48 Na^{+} cations) shows that nonspecific charge screening effects associated with the higher ion concentration are not enough to stabilize the catalytically active conformation of the pocket. Hence, the structural Mg^{2+} cations bound to specific phosphate sites on the backbone of the residues bridging the opposite strands of the pocket facilitate the catalytically competent open state of the catalytic pocket, as can be clearly seen in the simulations with eight Mg^{2+} ions in crystallographic positions plus an additional two noncrystallographic Mg^{2+} ions bridging phosphate groups of the 5′-G1-G2-A3-G4 segment.

The present results concerning the structural role of Mg^{2+} ions in enabling Diels−Alderase ribozyme function are in qualitative agreement with recent MD studies of the hammerhead ribozyme, which revealed a structural role of a Mg^{2+} ion bridging phosphate groups in the active site and thus stabilizing the catalytically competent conformation.[40−42] The Mg^{2+} ion was found to preserve the integrity of the active-site structure, allowing catalysis to proceed.[40] A striking result was the spontaneous migration of a Mg^{2+} ion to the bridging position between adenosine 9 and the scissile phosphate.[41] The most recent paper of this series uses MD and quantum mechanics/molecular mechanics (QM/MM) to provide evidence for facilitation of active conformations by Mg^{2+} ions stabilizing repulsions between negatively charged groups in the active site.[42] Furthermore, these studies provide evidence for a threshold cation occupation in the active site required for the formation of catalytically active conformations. In the case of the hammerhead ribozyme, the Mg^{2+} ions not only carry out structural roles but also are chemically involved in the catalysis by acting as Lewis acid catalysts, while there is no evidence for the direct involvement of metal ions in the reaction catalyzed by the Diels−Alderase ribozyme.[11]

The free energy profile of the catalytic pocket height, obtained from the simulations in solution at different Mg^{2+} ion concentrations, shows that with eight Mg^{2+} ions the free-energy minimum is at a closed state. In contrast, with 24 Mg^{2+} ions two states are seen: one closed and one open. These two states have similar energies and are separated by only a small barrier (5.5 kJ/mol), permitting frequent transitions between them. The concentration of 54 mM Mg^{2+} ions thus significantly increases the probability of the catalytic pocket being in the open-state conformation. The tertiary structure of the ribozyme remains catalytically active (i.e., able to host a reactant in the open catalytic pocket) only at high Mg^{2+} ion concentrations.

The hydrogen-bond analysis reveals that there is a competition between hydrogen bonding within the pocket and stabilization of the backbone of the residues from the 5′-G1-G2-A3-G4 segment. These residues play a key role in shaping both the RNA scaffold and the catalytic pocket. When the stabilization of the catalytically active open conformation is weak, the pocket collapses and the hydrogen bonds rearrange in such a way to prevent reopening if the concentration of the Mg^{2+} ions is too low. At the concentration of 54 mM Mg^{2+} ions, the interactions between the Mg^{2+} cations and the phosphorus atoms from the 5′-G1-G2-A3-G4 segment backbone are strong enough to break the rearranged hydrogen bonds, leading to reopening of the catalytic pocket.

Conclusions

The dynamic nature of the whole ribozyme in general and of the catalytic pocket region in particular is visible on the submicrosecond time scale. Although even at high Mg^{2+} ion concentrations the inactive, closed catalytic pocket state is the more probable, a second metastable state, with an open pocket that is catalytically active, is also populated. Selection of this nonglobal minimum conformation leads to activity of the Diels−Alderase ribozyme. It is the local conformation of the catalytic pocket that mainly determines whether the ribozyme can host its substrates and thus is active, as long as the global tertiary fold is maintained. These observations explain on the atomic level why the ribozyme achieves maximal catalytic efficiency at high Mg^{2+} ion concentrations: at too low Mg^{2+} ion concentrations, the catalytic pocket is unlikely to be intact, rendering the ribozyme unable to host the substrates.

Acknowledgment. T.B. thanks Emal M. Alekozai, Thomas Splettstoesser, and Lars Meinhold for useful discussions. We gratefully acknowledge funding from the German Research Foundation (DFG) through the award of a doctoral scholarship in the International Research Training Group IGK 710 "Complex Processes: Modeling, Simulation and Optimization". P.I. is grateful to the Landesstiftung Baden-Württemberg for funding in the Postdoctoral Elite Program. J.C.S. was supported by a Laboratory Directed Research and Development "Systems Biology" grant from the U.S. Department of Energy. The simulations were run on the Heidelberg Linux Cluster System at the Interdisciplinary Center for Scientific Computing (IWR) of the University of Heidelberg. The work was also supported by a National Science Foundation TeraGrid allocation provided by the National Institute for Computational Sciences.

Supporting Information Available: Crystal-state MD results: two tables, listing crystal unit cell properties and height and volume of the catalytic pocket, and two figures, showing temperature effect on the stability of the catalytic pocket, and structural fluctuations of the ribozyme. Solution MD results: two figures, showing magnesium ion dependent structural flexibility and free energy profiles in different environments, temperatures, and Mg^{2+} ion concentrations, and one table, listing interaction energies and distances between Mg^{2+} ions and phosphate groups from the 5′-G1-G2-A3-G4 segment. This material is available free of charge via the Internet at http://pubs.acs.org.

JA101370E

(40) Lee, T.-S.; López, C. S.; Martick, M.; Scott, W. G.; York, D. M. *J. Chem. Theory Comput.* **2007**, *3*, 325–327.
(41) Lee, T.-S.; López, C. S.; Giambasu, G. M.; Martick, M.; Scott, W. G.; York, D. M. *J. Am. Chem. Soc.* **2008**, *130*, 3053–3064.
(42) Lee, T.-S.; Giambasu, G. M.; Sosa, C. P.; Martick, M.; Scott, W. G.; York, D. M. *J. Mol. Biol.* **2009**, *388*, 195–206.